Dynamical Model of Prominence Formation and Oscillation (I)

J. Sakai[1, 2], A. Colin[2]
E. Priest[2]

1 Department of Applied Mathematics and Physics,
Faculty of Engineering,
Toyama University,
Toyama, 930 JAPAN

2 Department of Applied Mathematics,
University of St Andrews,
St Andrews, KY16 9SS,
Scotland, U. K.

Abstract

We investigate a dynamical model of prominence formation in a current sheet at the boundary between two regions of opposite magnetic polarity. Coupled nonlinear equations describing the temporal compression and condensation of plasma in the current sheet are set up as a natural extension of the usual equations for current sheet collapse (Imshennik and Syrovatskii, 1967). It is shown that under certain conditions the current sheet undergoes a nonlinear oscillation during the compression. The thermal instability with cooling is driven by a density enhancement produced during the current sheet formation stage.

1 Introduction

Observations of quiescent prominences indicate that they can form at the boundary between two weak magnetic regions of opposite polarity which are moving together (Martin, 1973; Tang, 1987). Stimulated by the observations, various kinds of model for quiescent prominences have been proposed (Tandberg-Hanssen, 1974; Priest, 1982; Hirayama, 1985).

Recently Malherbe et. al. (1983) and Schmieder et. al. (1984) have shown that slow upward motions ($v \cong 0.5$ km/s in Hα and 5–6 km/s in C$_{IV}$) can occur inside prominences and a fast input of material with horizontal motions ($v \cong 5$ km/s) can occur at both edges of a prominence, although in general the reported flows are still puzzling. Furthermore, Priest (1986) has suggested that prominences form at the boundary of two giant cells or approaching unipolar regions and Martin et. al. (1987) have proposed that, within such a global pattern, magnetic flux is continually brought into contact at network junctions where it produces cancelling magnetic features in photospheric magnetograms and provides a site for prominence formation in the overlying reconnecting current sheet.

The early models of solar prominences such as those due to Kippenhahn and Schlüter (KS) (1957) and Kuperus and Raadu (KR) (1974) are purely magnetostatic and do not take into

account the plasma dynamics. Malherbe and Priest (1983) and Malherbe et. (1983) proposed a qualitative dynamical model with magnetic configurations either of the KR or KS type to explain the observed upward motions, while Priest and Smith (1979) had previously suggested a dynamic arcade model with plasma dribbling through the magnetic field and being continually replaced by new plasma sucked up from the sides. Sakai and Washimi (1985) presented a general scheme to describe the dynamical behaviour of a current sheet.

The problem of the dynamics of current sheets has been one of great importance in connection with magnetic reconnection (see, for example, Priest (1985)). After the pioneering work of Dungey (1953), Imshennik and Syrovatskii (1967) investigated the non-steady collapse of an X point towards a current sheet. They used the two-dimensional time-dependent MHD equations with the density (p) assumed constant and the pressure gradient absent. Recently, an extension of this work has been achieved by Bulanov et. al. (1984), Sakai and Tajima (1986), and Sakai and Washimi (1985). Furthermore, Smith and Priest (1977) had presented a qualitative model for prominence condensation in a current sheet.

In the present paper we investigate the nonsteady dynamics of a current sheet, which might form at the boundary between two weak magnetic regions of opposite polarity (Figure 1), Following Imshennik and Syrovatskii (1967) and Sakai and Washimi (1985), we concentrate on the local behaviour of a current sheet produced by the approach of such magnetic regions.

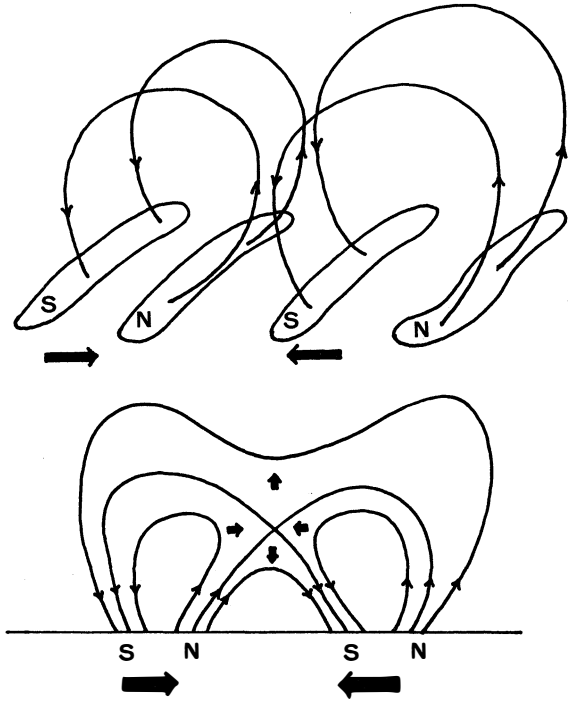

Fig. 1 Magnetic structure in the formation region of quiescent prominences. A current sheet may form at the boundary between two weak magnetic regions of opposite polarity moving together.

In section 2 we present the basic MHD equations and an enerey equation. We look for self-similar solutions describing plasma compression near the current sheet, which may eventually trigger a thermal instability condensation. The result is a set of coupled nonlinear ordinary differential equations.

In section 3 the nonlinear dynamics characterising the plasma condensation is investigated by analogy with the motions of a test particle under a given effective potential. We find in some cases a dynamical oscillation of the current sheet and in others a magnetic collapse (Sakai and Tajima, 1986; Tajima et. al., 1987).

In Section 4 we investigate some simplified cases and estimate the period of the nonlinear oscillation. An up-flow motion is generated. In Section 5 we discuss the nonlinear stage of the thermal instability which may be triggered when the density enhancement becomes too large. Finally, we summarise our results.

2 Basic Equations and Current Sheet Model

2.1 MHD Equations and Energy equation

We model a prominence as a vertical thin current sheet supported by the magnetic field in the low corona, as shown in Figure 2. The x-axis is chosen in the vertical direction,

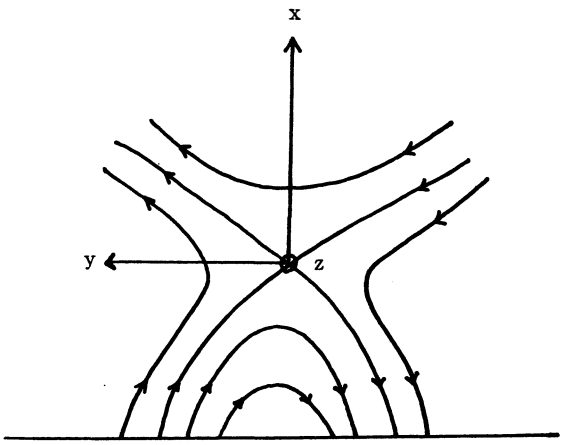

Fig. 2 Coordinates taken. The sheet is assumed homogenous in the horizontal z-direction.

the y-axis in the horizontal transverse direction, and the sheet is assumed homogenous in the horizontal z-direction along the prominence.

The theory of prominence formation may include several physical processes such as plasma compression dynamics, thermal and gravitational effects, coronal heating, radiation processes and magnetic reconnection. The relevant equations describing them are the MHD equations including gravity and an energy transport as follows:

$$\frac{\partial \rho}{\partial t} + \nabla \cdot (\rho \boldsymbol{V}) = 0, \tag{1.1}$$

$$\rho\left(\frac{\partial \boldsymbol{V}}{\partial t}+\boldsymbol{V}\cdot\nabla\boldsymbol{V}\right)=-\nabla P+\frac{1}{4\pi}(\nabla\times\boldsymbol{B})\times\boldsymbol{B}-\rho g\boldsymbol{e}_x, \tag{1.2}$$

$$\frac{\partial \boldsymbol{B}}{\partial t}=\nabla\times(\boldsymbol{V}\times\boldsymbol{B})+\frac{c^2}{4\pi\sigma}\Delta\boldsymbol{B}, \tag{1.3}$$

$$\frac{\partial P}{\partial t}+(\boldsymbol{V}\cdot\nabla)P+\gamma P\nabla\cdot\boldsymbol{V}=(\gamma-1)[E_H-Q_C+\nabla(\kappa_0 T^{5/2}\nabla T)], \tag{1.4}$$

where ρ, $\boldsymbol{V}$, P, $\boldsymbol{B}$ and T are the density, velocity, pressure, magnetic field and temperature, respectively, and γ is the adiabatic constant. The gravitational acceleration is given by

$$g(x)=GM_\odot R_\odot^{-2}\left(1+\frac{x}{R_\odot^2}\right)^{-2}=g_\odot\left(1+\frac{x}{R_\odot^2}\right)^{-2}, \tag{1.5}$$

where $M_\odot$, $R_\odot$ and $g_\odot=GM_\odot R_\odot^{-2}$ are the solar mass, solar radius and gravitational acceleration at the solar surface, respectively.

E_H and Q_C are the mechanical heating term and radiative cooling term, respectively, The heating term E_H due to waves or current dissipation is still not well-known. It is often assumed for simplicity to take the form

$$E_H=h\rho, \tag{1.6}$$

where h is a constant (see Priest, 1982, p 89). The radiative term is simply taken as

$$Q_C=\chi\rho^2T^\alpha, \tag{1.7}$$

where χ and α are constants; however, the temperature variation of the piecewise constants $\chi(T)$ and $\alpha(T)$ is given by, for example, Rosner et. al. (1978) and Priest (1982, pp 87−89).

In a magnetic field that is strong enough to make the thermal conduction perpendicular to the magnetic field negligible, the heat conduction term may be taken as $\nabla\cdot(\kappa_{11}\nabla_{11}T)$ in equation (1.4), where κ_{11} has the form $\kappa_{11}=\kappa_0 T^{5/2}$ (Spitzer, 1962).

2.2 Current Sheet Dynamics

We consider here a situation in which two magnetic regions of opposite polarity are approaching together as in Figure 1. An X-type magnetic configuration with current flowing in the z-direction could be formed by a horizontal plasma inflow from both sides. The horizontal plasma flow v_y around the X-type magnetic configuration is assumed to obey

$$v_y=\frac{\dot{a}}{a}y, \tag{2.1}$$

where a(t) is a time-dependent scale factor and $\dot{a}=da/dt$. The scale factor a(t), which is determined later, characterizes a continuous change of thickness of the current sheet.

The vertical flow v_x is taken to be

$$v_x=v_{x0}(t)+\frac{\dot{b}}{b}x, \tag{2.2}$$

where $v_{x0}(t)$ and another scale factor b(t) are determined self-consistently later.

The magnetic field components are assumed to take the form

$$B_x = B_{x0}(t)\frac{y}{\lambda}, \tag{2.3}$$

$$B_y = B_{n0}(t) + B_{y0(t)}\frac{x}{\lambda}, \tag{2.4}$$

$$B_z = B_{z0}(t), \tag{2.5}$$

where λ is a characteristic scale-length of the current sheet. Unknown functions such as $B_{x0}(t)$, $B_{n0}(t)$, $B_{y0}(t)$ and $B_{z0}(t)$ are also determined self-consistently later. The role of $B_{n0}(t)$ in Eq. (2.4) is to allow the X-point to move up or down during the current formation stage.

Substituting eqs. (2.1) and (2.2) into eq. (1.1), we find that the density $\rho(t)$ is only a function of time and

$$\frac{\dot{\rho}}{\rho} + \frac{\dot{a}}{a} + \frac{\dot{b}}{b} = 0, \tag{2.6}$$

which implies that

$$\rho(t) = \frac{\rho_0}{a(t)\,b(t)}, \tag{2.7}$$

where ρ_0 is a constant.

From the induction eq. (1.3), using the expression for magnetic fields ((2.3) −(2.5)) and velocities ((2.1) − (2.2)) we obtain

$$B_{x0}(t) = \frac{B_0}{a^2}, \tag{2.8}$$

$$B_{y0}(t) = \frac{B_0}{b^2}, \tag{2.9}$$

$$B_{z0}(t) = \frac{B_{00}}{a\,b}, \tag{2.10}$$

$$\frac{dB_{n0}}{dt} + \frac{v_{x0}}{\lambda}\frac{B_0}{b^2} + B_{n0}\frac{b}{b} = 0, \tag{2.11}$$

where B_0 and B_{00} are constants.

We assume the pressure P (x, y, t) to be

$$P(x,y,t) = P_{00}(t) - P_0(t)\frac{x}{\lambda} - P_{x0}(t)\frac{x^2}{\lambda^2} - P_{y0}(t)\frac{y^2}{\lambda^2}, \tag{2.12}$$

and next substitute equations (2.1) − (2.5), (2.7), (2.8) − (2.10) and (2.12) into the equation of motion (1.2). The term proportional to x^0 in the x-component gives

$$\frac{dv_{x0}}{dt} + \frac{\dot{b}}{b}v_{x0} = \frac{a\,b\,P_0(t)}{\lambda\rho_0} - \frac{B_0 B_{n0}\,a\,b}{4\pi\rho_0\lambda}\left(\frac{1}{b^2} - \frac{1}{a^2}\right) - g_\odot, \tag{2.13}$$

while the term proportional to x gives

$$\frac{d^2b}{dt^2} = \frac{2P_{x0}a\,b^2}{\lambda^2\rho_0} - \frac{v_A^2}{\lambda^2}\left(\frac{a}{b^2} - \frac{1}{a}\right) + 2\frac{g_\odot}{R_\odot}b, \tag{2.14}$$

where $v_A^2 = B_0^2/4\pi\rho_0$

Similarly the y-component of eq. (1.2) implies

$$\frac{d^2a}{dt^2}=\frac{2P_{y0}a^2b}{\lambda^2\rho_0}+\frac{v_A^2}{\lambda^2}\left(\frac{1}{b}-\frac{b}{a^2}\right). \tag{2.15}$$

Finally we examine the energy equation (1.4), in which the heating term and radiative loss term are given by (1.6) and (1.7), respectively. From the equation of state, $P=nk_BT=\rho k_BT/M$ where M is the proton mass, we find

$$T(x,y,t)=\frac{MP}{k_B\rho}=\frac{Mab}{k_B\rho_0}\left(P_{00}(t)-P_0(t)\frac{x}{\lambda}-P_{x0}(t)\frac{x^2}{\lambda^2}-P_{y0}(t)\frac{y^2}{\lambda^2}\right), \tag{2.16}$$

after using eqs. (2.7) and (2.12).

A Taylor expansion of expressions for $P^{5/2}$ and P^{α} gives

$$\left.\begin{aligned}P^{5/2}&\cong P_{00}^{5/2}\left(1-\frac{5}{2}\frac{P_0}{P_{00}}\frac{x}{\lambda}-\frac{5}{2}\frac{P_{x0}}{P_{00}}\frac{x^2}{\lambda^2}-\frac{5}{2}\frac{P_{y0}}{P_{00}}\frac{y^2}{\lambda^2}\right),\\ P^{\alpha}&\cong P_{00}^{\alpha}\left(1-\alpha\frac{P_0}{P_{00}}\frac{x}{\lambda}-\alpha\frac{P_{x0}}{P_{00}}\frac{x^2}{\lambda^2}-\alpha\frac{P_{y0}}{P_{00}}\frac{y^2}{\lambda^2}\right).\end{aligned}\right\} \tag{2.17}$$

Then the terms proportional to x^0, x and x^2 in equation (1.4) give, respectively,

$$\frac{dP_{00}}{dt}-v_{x0}\frac{P_0}{\lambda}+\gamma P_{00}\left(\frac{\dot a}{a}+\frac{\dot b}{b}\right)=(\gamma-1)\left[\frac{h\rho_0}{ab}-\chi\rho_0^{2-\alpha}\left(\frac{M}{k_B}\right)^{\alpha}(ab)^{\alpha-2}P_{00}^{\alpha}\right.$$
$$\left.+\varkappa_0\left(\frac{M}{k_B\rho_0}\right)^{7/2}(ab)^{7/2}P_{00}^{5/2}\left\{\frac{5}{2}\frac{P_0^2}{\lambda^2P_{00}}-\frac{2P_{x0}}{\lambda^2}-\frac{2P_{y0}}{\lambda^2}\right\}\right], \tag{2.18}$$

$$\frac{dP_0}{dt}+\frac{\dot b}{b}P_0+2v_{x0}\frac{P_{x0}}{\lambda}+\gamma P_0\left(\frac{\dot a}{a}+\frac{\dot b}{b}\right)=-(\gamma-1)\left[\alpha\chi\rho_0^{2-\alpha}\left(\frac{M}{k_B}\right)^{\alpha}(ab)^{\alpha-2}P_0P_{00}^{\alpha-1}\right.$$
$$\left.+\varkappa_0\left(\frac{M}{k_B\rho_0}\right)^{7/2}(ab)^{7/2}P_{00}^{5/2}\left\{15\frac{P_0P_{x0}}{P_{00}\lambda^2}+5\frac{P_0P_{y0}}{P_{00}\lambda^2}\right\}\right], \tag{2.19}$$

$$\frac{dP_{x0}}{dt}+\left\{\gamma\frac{\dot a}{a}+(\gamma+2)\frac{\dot b}{b}\right\}P_{x0}=-(\gamma-1)\left[\alpha\chi\rho_0^{2-\alpha}\left(\frac{M}{k_B}\right)^{\alpha}(ab)^{\alpha-2}P_{x0}P_{00}^{\alpha-1}\right.$$
$$\left.+\varkappa_0\left(\frac{M}{k_B\rho_0}\right)^{7/2}(ab)^{7/2}P_{00}^{5/2}\left\{15\frac{P_{x0}^2}{P_{00}\lambda^2}+5\frac{P_{x0}P_{y0}}{P_{00}\lambda^2}\right\}\right], \tag{2.20}$$

while the term proportional to y^2 implies

$$\frac{dP_{y0}}{dt}+\left\{(\gamma+2)\frac{\dot a}{a}+\gamma\frac{\dot b}{b}\right\}P_{y0}=-(\gamma-1)\left[\alpha\chi\rho_0^{2-\alpha}\left(\frac{M}{k_B}\right)^{\alpha}(ab)^{\alpha-2}P_{y0}P_{00}^{\alpha-1}\right. \tag{2.21}$$
$$\left.+\varkappa_0\left(\frac{M}{k_B\rho_0}\right)^{7/2}(ab)^{7/2}P_{00}^{5/2}\left\{15\frac{P_{y0}^2}{P_{00}\lambda^2}+5\frac{P_{x0}P_{y0}}{P_{00}\lambda^2}\right\}\right].$$

The basic equations describing the current sheet dynamics have thus been derived, namely eqs. (2.11), (2.13), (2.14), (2.15), (2.18), (2.19) and (2.21).

If we assume in particular an adiabatic compression in eqs. (2.18) – (2.21) they reduce to

$$\frac{dP_{00}}{dt}-v_{x0}\frac{P_0}{\lambda}+\gamma P_{00}\left(\frac{\dot a}{a}+\frac{\dot b}{b}\right)=0, \tag{2.22}$$

$$\frac{dP_0}{dt}+\frac{\dot b}{b}P_0+2v_{x0}\frac{P_{x0}}{\lambda}+\gamma P_0\left(\frac{\dot a}{a}+\frac{\dot b}{b}\right)=0, \tag{2.23}$$

$$P_{x0}=\frac{P_a}{a^{\gamma}b^{\gamma+2}}, \tag{2.24}$$

$$P_{y0} = \frac{P_a}{a^{\gamma+2} b^{\gamma}} \tag{2.25}$$

where P_a is a constant

3. Adiabatic Compression

3.1 Lagrangian of the System

In the previous section we derived the basic equations for the current sheet formation. When the plasma compression occurs adiabatically, the reduced equations can be simplified since the basic equations describing the scale factors a and b ((2.14) and (2.15)) can be rewritten after using the relations (2.24) and (2.25) as

$$\frac{d^2 a}{dt^2} = \frac{c_s^2}{\lambda^2 a^{\gamma} b^{\gamma-1}} + \frac{v_A^2}{\lambda^2}\left(\frac{1}{b} - \frac{b}{a^2}\right), \tag{3.1}$$

$$\frac{d^2 b}{dt^2} = \frac{c_s^2}{\lambda^2 a^{\gamma-1} b^{\gamma}} - \frac{v_A^2}{\lambda^2}\left(\frac{a}{b^2} - \frac{1}{a}\right) + 2\frac{g_\odot}{R_\odot} b, \tag{3.2}$$

where $c_s^2 = 2P_a/\rho_0$

The above equations without the terms involving the effects of gravity and the plasma pressure were first derived by Imshennik and Syrovatskii (1967), who investigated current sheet dynamics in relation to solar flares.

Once the scale factors a(t) and b(t) are known, it is easy to see the time behaviour of physical quantities such as the magnetic field and velocity, So we first investigate the above equations (3.1) and (3.2) from a general point of view. They can be derived from the Euler-Lagrange equations

$$\frac{d}{dt}\left(\frac{\partial L}{\partial \dot{a}}\right) = \frac{\partial L}{\partial a}, \tag{3.3}$$

$$\frac{d}{dt}\left(\frac{\partial L}{\partial \dot{b}}\right) = \frac{\partial L}{\partial b}, \tag{3.4}$$

where the Lagrangian $L(a, \dot{a}, b, \dot{b})$ is given by

$$L(a, \dot{a}, b, \dot{b}) = \frac{\dot{a}^2}{2} + \frac{\dot{b}^2}{2} + \frac{v_A^2}{\lambda^2}\left(\frac{b}{a} + \frac{a}{b}\right) + \frac{g_\odot}{R_\odot} b^2 - \frac{c_s^2}{(\gamma-1)\lambda^2 (ab)^{\gamma-1}}. \tag{3.5}$$

The first two terms correspond to kinetic energy T_K, by analogy with the mechanical system of a test particle in a potential well

$$T_K = \frac{\dot{a}^2}{2} + \frac{\dot{b}^2}{2}, \tag{3.6}$$

and the remaining terms correspond to an effective potential

$$V_{eff} = -\frac{v_A^2}{\lambda^2}\left(\frac{b}{a} + \frac{a}{b}\right) - \frac{g_\odot}{R_\odot} b^2 + \frac{c_s^2}{(\gamma-1)\lambda^2 (ab)^{\gamma-1}} \tag{3.7}$$

It is clear that the above system has a first integral, which is constant and corresponds to the total energy E_T of the mechanical system

$$E_T = T_K + V_{eff} = \frac{\dot{a}^2}{2} + \frac{\dot{b}^2}{2} - \frac{v_A^2}{\lambda^2}\left(\frac{b}{a} + \frac{a}{b}\right) - \frac{g_\odot}{R_\odot} b^2 + \frac{c_s^2}{(\gamma-1)\lambda^2 (ab)^{\gamma-1}}, \tag{3.8}$$

$$= \text{constant}.$$

3.2 Effective potential surface

By analogy with the motion of a test particle under the effective potential V_{eff} (Eq. (3.7 (3.7)), we can easily understand the dynamical behaviour of the scale factors a(t) and b (t) if we draw the effective potential. Here we consider the following normalized potential F(a, b), and examine its behaviour.

$$F(a,b) = \frac{\lambda^2}{v_A^2} V_{eff}$$

$$= -\left(\frac{b}{a} + \frac{a}{b}\right) - G_0 b^2 + \frac{\beta}{\Gamma (ab)^{\Gamma}}, \qquad (3.9)$$

where

$$G_0 = \frac{\lambda^2 g_\odot}{v_A^2 R_\odot}, \quad \beta = \frac{c_S^2}{v_A^2}, \quad \Gamma = \gamma - 1.$$

The second term in Eq. (3.9), which represents the effect of gravity, is negligible when the coefficient G_0 is taken to be 4×10^{-3} as a representative value in the solar corona. Then the function F(a, b) is almost symmetric with respect to the plane a =b, On the plane a =b the curve F(a =b) decreases monotonically from ∞ at a =b = 0 to $-\infty$, because

$$F(a=b) = -2 - G_0 a^2 + \frac{\beta}{\Gamma a^{2\Gamma}}, \qquad (3.10)$$

and

$$\frac{dF(a=b)}{da} = -2G_0 a - \frac{2\beta}{a^{2\Gamma-1}} < 0 . \qquad (3.11)$$

We have studied two examples of the potential F(a, b):

(a) $G_0 = 4 \times 10^{-3}$, $\beta = 0.01$, $\Gamma = 2$ ($\gamma = 3$)

(b) $G_0 = 4 \times 10^{-3}$, $\beta = 0.01$, $\Gamma = 2/3$ ($\gamma = 5/3$)

where we have set $\lambda / v_A = 10^2$sec, $g_\odot = 2.71 \times 10^4$ cm/sec^2, and $R_\odot = 6.96 \times 10^{10}$ cm.

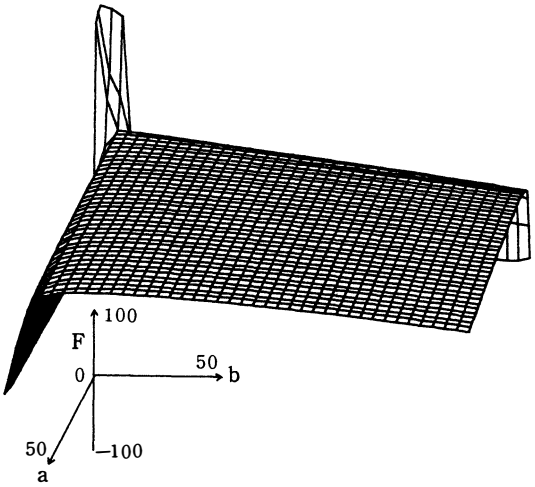

Fig 3. Effective Potential surface; F(a, b) when $G_0 = 4 \times 10^{-3}$, $\beta = 0.01$, $\Gamma = 2$ ($\gamma = 3$)

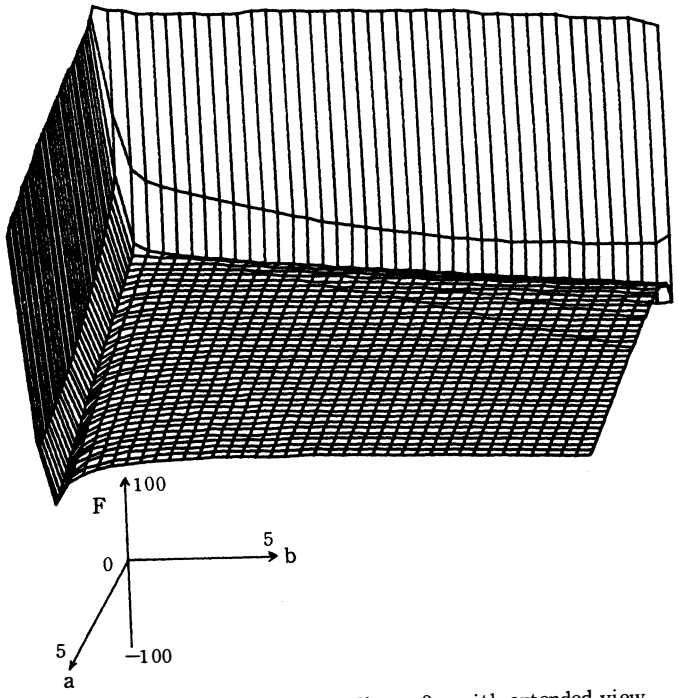

Fig. 4 Effective potential surface, as in Figure 3, with extended view around the origin.

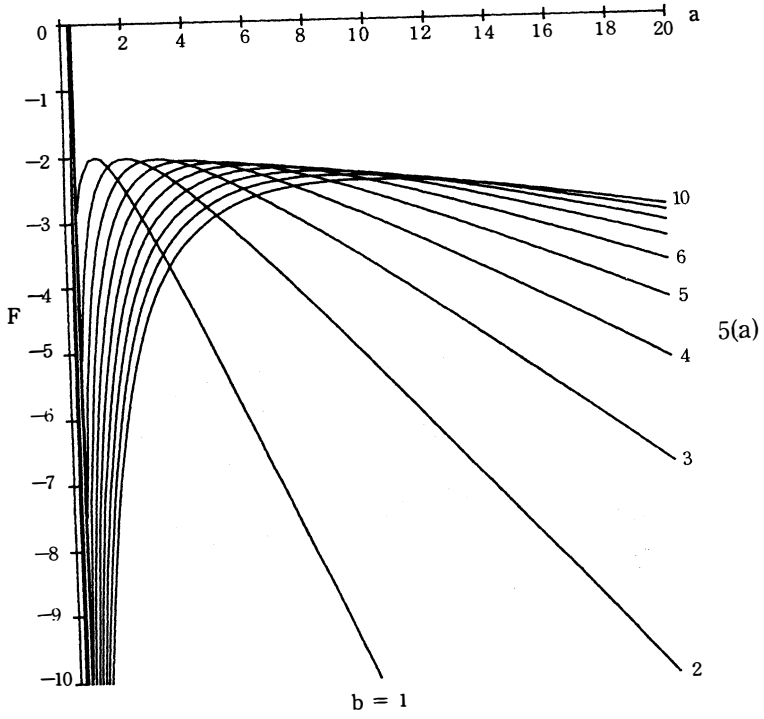

Fig. 5 Cross-sections of the potential: (a) F (a) for given b = 1 −10, and (b) F (b) for given a = 1 −10; same parameters as Fig. 3.

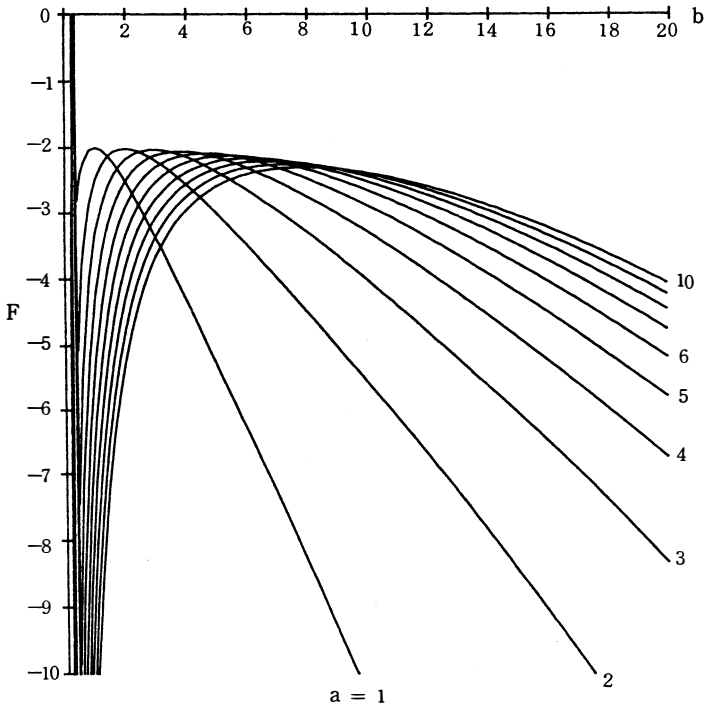

5(b)

Figures 3, 4 and 5 show the case (a), while Figures 6 and 7 show the case (b). As seen in Figures 3–5, there are deep potential wells (a potential minimum exists) near the planes a =0 and b =0 in case (a). On the other hand, in case (b) there is no potential well, but there exists a high wall near the origin (a = b = 0). Further, there is a deep potential drop reaching to $-\infty$ near the planes a = 0 and b = 0.

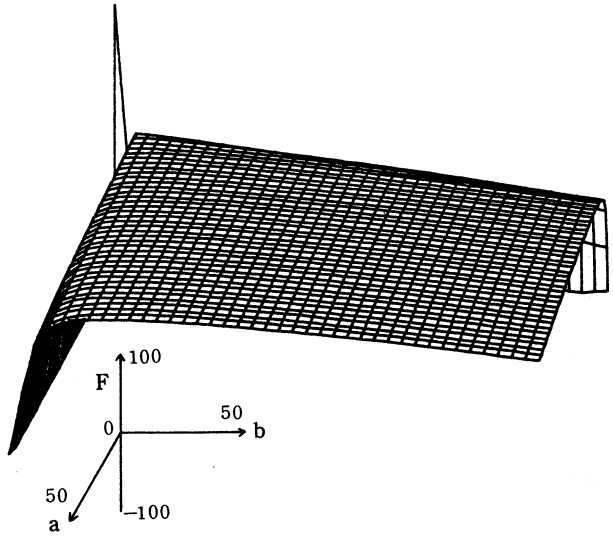

Fig 6. Effective potential surface; F(a, b) when $G_0 = 4 \times 10^{-3}$, $\beta = 0.01$, $\Gamma = 2/3$ ($\gamma = 5/3$)

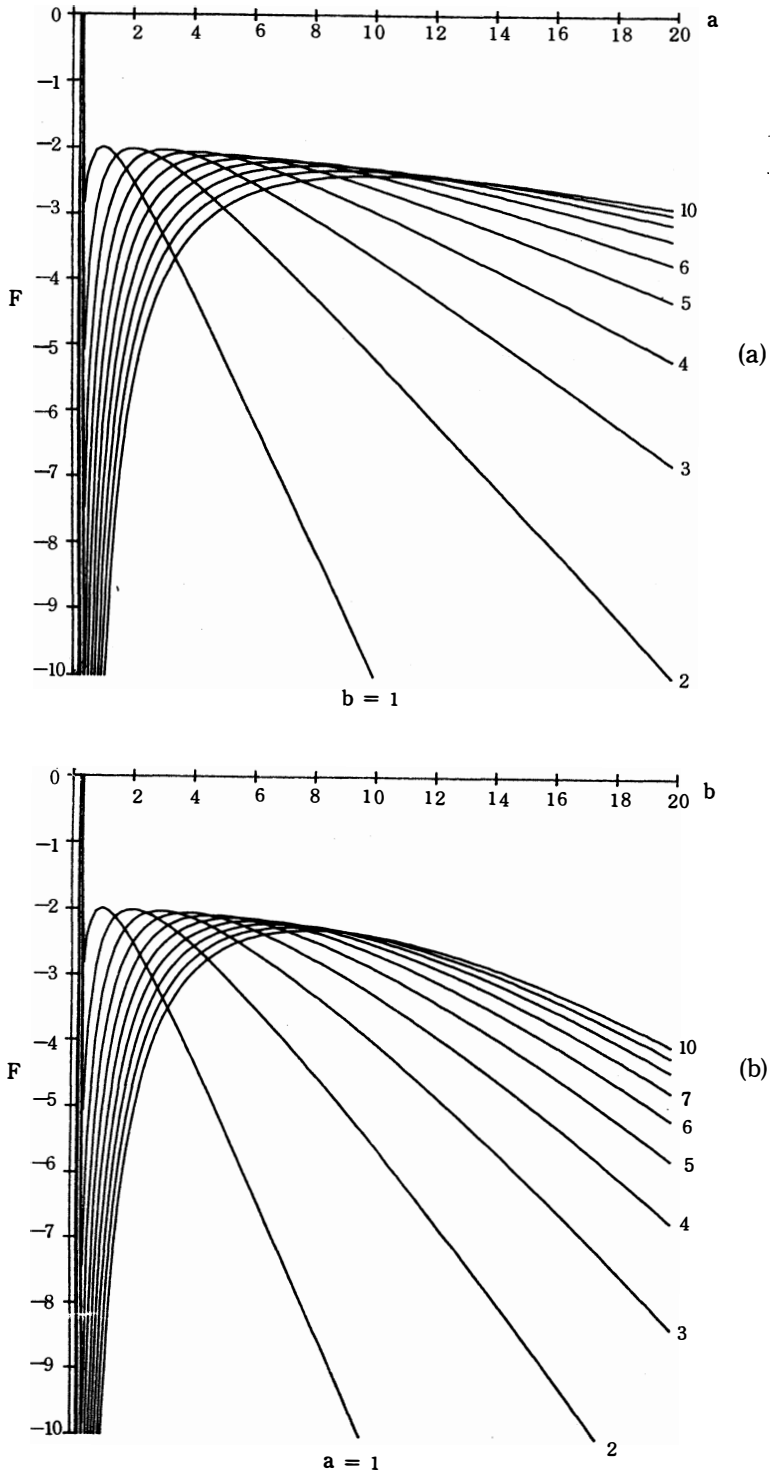

Fig 7. Cross-sections of the potential: (a) F(a) for given b = 1 −10, and (b) F(b) for given a = 1 −10; same parameters as Fig. 6.

The case (a) corresponds to the occurrence of a simple nonlinear oscillation, which will be investigated further in the next section.

On the other hand, we find only magnetic collapse driven by magnetic forces in case (b). Because of the high potential wall near the origin, the scale factors a and b may not decrease along the line a = b, but the scale factor a can decrease more rapidly than b during magnetic collapse. This implies that magnetic collapse may show a quasi-one-dimensional behaviour; i.e. $a \to 0$ and b is almost constant in time. We will investigate such a one-dimensional collapse in detail in section 5.

4. Current sheet oscillation and upflow motion

In the previous section we investigated in general the time-dependent behaviour of plasma compression by using the analogy of motion of a test particle in an effectiuve potential. We here study a special case, where the horizontal magnetic field B_y is a constant; $B_y = B_n =$ constant in Eq. (2.4). This magnetic configuration may be approximately realized in the X-type magnetic structure shown in Figure 2. It is also similar to the central part of the KS model, where the forces between magnetic tension (up) and gravity (down) balance. We can generalise the static KS model to a dynamic model including horizontal plasma flow as well as plasma up-flow.

The basic equation for the scale factor a(t), neglecting the inhomogeneous flow term in the x-direction in Eq. (2.2), and assuming an adiabatic compression, is then

$$\frac{d^2 a}{dt^2} = \frac{c_s^2}{\lambda^2 a^{\gamma}} - \frac{v_A^2}{\lambda^2 a^2} \quad . \tag{4.1}$$

The density, velocity and magnetic field follow form

$$\rho = \frac{\rho_0}{a} \quad , \tag{4.2}$$

$$v_y = \frac{\dot{a}}{a} y \quad , \tag{4.3}$$

$$B_x = \frac{B_0}{a^2} \frac{y}{\lambda} \, , \tag{4.4}$$

$$B_y = B_n = \text{constant}, \tag{4.5}$$

$$B_z = \frac{B_0}{a} \quad . \tag{4.6}$$

The up-flow velocity $v_{x0}(t)$ is determined by

$$\frac{dv_{x0}}{dt} = \frac{v_A^2 B_n}{\lambda B_0 a} - g \quad , \tag{4.7}$$

where the gravitational acceleration g is assumed to be constant in the current sheet. If the first term on the right-hand side of equation (4.7) is larger than the second gravity term, an up-flow motion ($v_{x0} > 0$) can occur, If a(t) becomes smaller than $a_0 = \frac{v_A^2 B_n}{\lambda B_0 g}$, plasma compression can lead to such an up-flow motion. Otherwise, if there does not occur enough compression ($a > a_0$), down-flow may exist in the prominence current sheet. We may thus have the possibility of a transition from up-flow to down-flow during the formation stage of

a prominence.

4.1 Nonlinear oscillation

In Eq. (4.1) with $\gamma > 2$, we find (Sakai and Tajima, 1986) a nonlinear oscillation with respect to a(t). It impies that the in-flow plasma velocity, $v_y = \frac{\dot{a}}{a} y$ as well as other physical quantities can undergo an oscillation in time. The period T of the oscillation is given by (Sakai and Tajima, 1986)

$$T = 2\pi v_A^2 / E_0^{3/2} \lambda^2, \tag{4.8}$$

where

$$E_0 = \dot{a}_0^2 - 2V_A^2 / \lambda a_0 + c_S^2 / \lambda^2 a_0^2 .$$

E_0 is related to the initial inflow velocity. The minimum period, when the amplitude of the oscillation is very small, is given by

$$T_{min} = 2\pi \beta^{3/2} \tau_A, \tag{4.9}$$

where $\tau_A = \lambda / v_A$, $\beta = c_S^2 / v_A^2$.

If we take $\lambda \sim 10^9$ cm, $v_A \sim 10^7$ cm/s and $\beta = 0.01$ we obtain $T_{min} \sim 0.6$ second. The nonlinear period T of the oscillation becoms longer than T_{min} by an amount that depends on the initial condition E_0.

4.2 Up-flow motion

When $\gamma < 2$ and $c_S < v_A$, Eq. (4.1) only gives a collapse solution without oscillation. The approximate solution in the case when $\gamma = 2$ and E_0 is close to zero is given by

$$a(t) = \left(\frac{9}{2}\right)^{1/3} (v_A^2 - c_A^2)^{1/3} \lambda^{-\frac{2}{3}} (t_0 - t)^{2/3}, \tag{4.10}$$

which gives the solution of Eq. (4.7) as

$$v_{x0}(t) = 3\left(\frac{2}{9}\right)^{1/3} \frac{v_A^2}{\lambda^{1/3}} \frac{B_n}{B_0} \frac{(t_0 - t)^{1/3}}{(v_A^2 - c_S^2)^{1/3}} - g(t_0 - t), \tag{4.11}$$

where t_0 is the time when $v_{x0} = 0$, t_0 is roughly given by

$$t_0 \cong 0.84 (v_A / c_S)^3 \tau_A,$$

which may be explained by the life-time of the up-flow motion. If we take, for example, $v_A / c_S \sim 10$, $\tau_A \sim 10^2$sec, we find $t_0 \cong 0.84 \times 10^5$s.

5 Condensation and Cooling

In the previous sections we found that the current sheet can undergo a magnetic collapse ($a \to 0$) driven by the $\boldsymbol{j} \times \boldsymbol{B}$ force. When $\gamma < 2$, the plasma compression can be suppressed by the build-up of an internal plasma pressure; while, for $\gamma < 2$, the plasma compression may still continue (i.e. we have a magnetic collapse). During the magnetic collapse ($a, b \to 0$) the plasma density $\rho = \rho_0 / ab$ in the current sheet is greatly enhanced. Then the radiative loss term which was neglected in the previous sections may become important in a phase

when the radiative cooling term in Eq. (1.7) proportional to ρ^2 dominates the heating and conduction terms in Eq. (1.4).

In the following we investigate one-dimensional condensation dynamics. The analysis is simpler than a fully 2-D situation, and in any case the 1-D dynamics themselves can often be a good approximation to the 2-D dynamics when the magnetic collapse occurs almost one-dimensionally as $a \to 0$ and $b \cong$ constant.

5.1 Basic equations for 1-D condensation

From the basic equations (1.1) – (1.7), we find the following relations and reduced nonlinear equations by a similar method to that used in the previous section:

$$\rho(y,t) = \frac{\rho_0}{a}, \tag{5.1}$$

$$v_y(y,t) = \frac{\dot{a}}{a} y, \tag{5.2}$$

$$B_x(y,t) = \frac{B_0}{a^2} \frac{y}{\lambda}, \tag{5.3}$$

$$B_z(t) = \frac{B_0}{a}, \tag{5.4}$$

$$P(y,t) = P_0(t) - P_1(t) \frac{y^2}{2\lambda^2}, \tag{5.5}$$

where $a(t)$, $P_0(t)$ and $P_1(t)$ are determined by

$$\frac{d^2 a}{dt^2} = \frac{a^2}{\rho_0 \lambda^2} P_1(t) - \frac{v_A^2}{a^2 \lambda^2}, \tag{5.6}$$

$$\frac{dP_1}{dt} + (\gamma+2) P_1 \frac{\dot{a}}{a} = -(\gamma-1) \frac{\alpha \chi \rho_0^2}{n_0^\alpha} a^{\alpha-2} P_0^{\alpha-1} P_1, \tag{5.7}$$

$$\frac{dP_0}{dt} + \gamma P_0 \frac{\dot{a}}{a} = (\gamma-1) \left[\frac{h\rho_0}{a} - \frac{\chi \rho_0^2 a^{\alpha-2} P_0^\alpha}{n_0^\alpha} + \frac{\kappa_0 T^{5/2} \Delta T}{\lambda_{11}^2} \right]. \tag{5.8}$$

In Eq. (5.8) we have introduced an order of magnitude term representing the effect of heat conduction parallel to the magnetic field B_y, Such a term gives a stabilizing effect against thermal instability and may be important when we are discussing the approach to and onset of thermal instability.

The plasma temperature $T(y, t)$ is determined by use of $p = nk_B T$ as

$$T(y, t) = T_0(t) - T_1(t) \frac{y^2}{2\lambda^2}, \tag{5.9}$$

where

$$T_0(t) = a P_0(t) / (n_0 k_B), \tag{5.10}$$

$$T_1(t) = a P_1(t) / (n_0 k_B). \tag{5.11}$$

5.2 Radiative Cooling

We here consider a phase in which the radiative cooling term in Eq. (5.8) becomes dominant,

when magnetic collapse ($a \to 0$) may lead to the relations

$$\frac{\chi \rho_0^2 a^{\alpha-2} P_0^{\alpha}}{\eta_0^{\alpha}} \gg \frac{h \rho_0}{a} \text{ and } \frac{\kappa_0 T^{5/2} \Delta T}{\lambda_{11}^2}$$

We find then the following asymptotic solutions for the physical quantities from Eqs. (5.6) – (5.8) :

$$a(\tau) \propto \tau^{\frac{2}{3}} , \tag{5.12}$$

$$\rho(\tau) \propto \tau^{-\frac{2}{3}} , \tag{5.13}$$

$$v_y(\tau) \propto \tau^{-1} , \tag{5.14}$$

$$B_x(\tau) \propto \tau^{-4/3} , \tag{5.15}$$

$$P_0(\tau) \propto \tau^{k} , \tag{5.16}$$

$$P_1(\tau) \propto \tau^{-8/3} , \tag{5.17}$$

$$T_0(\tau) \propto \tau^{l} , \tag{5.18}$$

$$T_1(\tau) \propto \tau^{-2} , \tag{5.19}$$

where

$$k = \frac{2\alpha - 1}{3(1-\alpha)} , \tag{5.20}$$

$$l = \frac{1}{3(1-\alpha)} , \tag{5.21}$$

$$\tau = t_0 - t . \tag{5.22}$$

From Eq. (5.18), we find that plasma compression ($a \to 0$ as $\tau \to 0$) can produce plasma cooling ($T_0 \propto \tau^{l} \to 0$) near the centre of the current sheet, provided $l > 0$. The condition $l > 0$ for cooling to occur can be realized in the case

$$\alpha < 1 , \tag{5.23}$$

from Eq. (5.21)

We may conclude from the above discussion that the current sheet becomes dense and cool due to the effect of radiative loss, following the magnetic collapse of the current sheet. Of course, eventually when the temperature becomes much cooler than 10^5 K and α exceeds unity, we expect the fall in temperature to be slowed and to cease as a new cool equilibrium at prominence temperatures is attained.

6 Conclusions

We have investigated a dynamical model for prominence formation in a current sheet at the boundary between regions of opposite magnetic polarity. We have derived a set of coupled nonlinear equations describing the temporal compression and condensation of plasma in the current sheet with gravity, heating, radiative cooling and heat conduction included.

The dynamics of magnetic collapse has been investigated and shown to produce a nonlinear oscillation of the current sheet and up-flow motion. Also, an asymptotic solution describing radiative cooling and plasma compression in a 1−D current sheet configuration was presented. In future it is hoped to study the problem further by solving both the 1−D and 2−D equations numerically.

Acknowledgements

We are grateful to the UK Science and Engineering Research Council for supporting this work.

J.S. is grateful to the Japan Society for the Promotion of Science and to the Royal Society for supporting his visit to St Andrews.

この研究の一部は，財団法人富山相銀奨学育英財団によって援助されたことを記し感謝の意を表わす。

References

Bulanov, S.V. and Ol' Shanetskij. M.A.: 1984, Phys. Lett., **100**A, 35

Dungey, J.W., Philosoph. Mag.: 1953, **44**, 725

Hirayama, T.: 1985, Solar Phys., **100**, 415

Imshennik, V.S., Syrovatskii, S.I.: 1967, Soviet Phys. JETP, **25**, 656

Kippenhahn, R., Schlüter, A.: 1957, Z. Astrophys., **43**, 36

Kuperus, M., Raadu, M.A.: 1974, Astron. Astrophys, **31**, 189

Malherbe, J.M., Priest E.R.: 1983, Astron. Astrophys., **127**, 80

Malherbe, J.M., Priest, E·R., Forbes, T.G., Heyvaerts, J.: 1983, Astron. Astrophys., **127**, 153

Malherbe, J.M., Schmieder, B., Ribe, E., Mein, P.: 1983, Asstron, Astrophys., **119**, 197

Martin, S.F.: 1973, Solar Phys., **31**, 3

Martin, S.F., Liv, S.H.B., Wang J.: 1985, Australian J. Phys, **38**, 929

Martin, S.F.: 1987, Proc. of Coronal and Prominence Plasmas, NASA Conference Publication 2442

Priest, E.R.: 1982, Solar Magnetohydrodynamics, Reidel Publ. Co., Dordrecht, Holland

Priest, E.R.: 1985, Rep. Prog. Phys., **48**, 955

Priest, E.R., Smith.E.A.: 1979, Solar Phys, **64**, 267

Priest, E.R.: 1986, in The Role of Fine-Scale Magnetic Fields on sthe Structure of the Solar Atmosphere, Proc. Tenerife Workshop, Octoaber (in press)

Rosner, R., Tucker, W.H., Viana, G.S.: 1978, Astrophys. J., **220**, 643

Sakai, J., Tajima, T.: 1986, Proc. on Plasma Astrophysics, ESA SP−251, 77

Sakai, J., Washimi, H.: 1985, Bulletin of Faculty of Engineering, Toyama University, **36**, 47

Schmieder, B., Malherbe, J.M., Ribes, E., Mein, P.: 1984, Astron. Astrophys,, **136**, 81

Smith, E.A., Priest, E.R.: 1977, Solar Phys., **53**, 25

Spitzer, L.: 1962, Physics of Fully Ionized Gases, Interscience, New York

Tajima, T., Sakai, J.: 1986, IEEE Transactions on Plasma Science, PS−14, **6**, 929

Tajima, T., Sakai, J., Nakajima, H., Kosugi, T., Brunel, F., Kundu, M.R.: 1987, Astrophys. J. 321, 1031.

Tandberg-Hanssen, E.: 1974, Solar Prominences, D. Reidel Publ. Co., Dordrecht, Holland

Tang, F.: 1987, Solar Phys., **107**, 233

(Received October, 30 1987)